AUIQ Technical Engineering Science

Manuscript 1040

Assessment of the Thermal Performance of Cables at Zummar Station, Considering the Impact of Harmonics

Riyad Zaki Sabri Younis

Khaled Mohammed Othman

Follow this and additional works at: https://ates.alayen.edu.iq/home



Part of the Engineering Commons



Scan the QR to view the full-text article on the journal website

Assessment of the Thermal Performance of Cables at Zummar Station, Considering the Impact of Harmonics

Riyad Zaki Sabri Younis, Khaled Mohammed Othman *

College of Engineering, Department of Electrical Engineering, University of Mosul, Iraq

ABSTRACT

This study evaluates the thermal impact of harmonic distortion on underground power cables through a real-life case study conducted at the Zummar 33/11 kV substation. Field measurements indicated that the cable most exposed to thermal stress was the one supplying an industrial area, where a Total Harmonic Distortion (THD) level of 23.8% was recorded due to nonlinear loads. Numerical simulations were carried out using the Finite Element Method (FEM) to analyze the thermal performance of the cable system under different seasonal loading conditions. The results showed that harmonics not only increased the temperature of the affected cable but also indirectly raised the temperatures of adjacent cables, leading to partial thermal redistribution within the system. These findings highlight the importance of integrating harmonic analysis with thermal modeling to achieve accurate current rating assessments and ensure the safe and efficient design of underground power cables, particularly in substations supplying nonlinear industrial loads.

Keywords: Power cable, harmonic, Ampacity, Thermal analysis, backfilling material, Thermal performance of underground power cables

1. Introduction

The increasing demand for electric power, among other factors, has led to the expanded use of power cables [1-3]. In areas such as city centers, overhead lines are often undesirable or even impractical; therefore, underground cables are widely used for electric power transmission [4, 5]. The proper selection of cable size, insulation type, and number of insulation layers significantly affects the cable's currentcarrying capacity (ampacity), and improving the cable's thermal performance substantially enhances system reliability [6]. The conductor's cross-sectional area, electrical conductivity, and operating temperature are the primary determinants of the cable's ampacity, or the maximum safe current. While direct current (DC) cables follow a linear relationship between cross-section and ampacity, alternating current

(AC) cables behave differently due to non-uniform current density distribution caused by electromagnetic phenomena such as the skin and proximity effects. The current flowing through the conductor generates heat, which raises its temperature and affects the surrounding insulation. Long-term exposure to high temperatures can lead to insulation deterioration and permanent cable failure [7–9]. Assuming uniform soil conditions with consistent thermal characteristics, international standards such as IEEE and IEC provide methods for calculating cable current ratings, conductor and insulation resistance, and the thermal resistance between the cable system and its surroundings [10, 11]. During real-time operation, the soil around the buried cable tends to dry and heat up, which reduces its thermal conductivity and directly affects the cable system's ability to dissipate heat [12, 13]. To ensure effective and long-lasting

Received 16 June 2025; revised 8 August 2025; accepted 9 August 2025. Available online 26 August 2025

Corresponding author.

E-mail addresses: electricity@uomosul.edu.iq (R. Z. Sabri Younis), Khaled.osmany994@gmail.com (K. M. Othman).

operation of underground cable systems, heat must be transferred from the conductor through the structural layers of the cable into the surrounding soil [14]. Increasing the spacing between underground cables helps prevent thermal accumulation, and altering cable configurations can reduce heat retention. For example, flat arrangements offer higher ampacity than trefoil arrangements due to improved heat dissipation [15]. Ambient temperature is another crucial factor in conductor cooling; as it rises, the cable's ability to dissipate heat decreases, thereby reducing its current-carrying capacity [16]. Nonlinear loads, such as power electronics and induction furnaces, are commonly used in industrial and urban environments. Consequently, the presence of high-frequency components produced by such loads has made harmonic distortion a critical concern [17, 18]. Total harmonic distortion (THD) often exceeds the acceptable limits set by IEEE 519-1992 in residential, commercial, and industrial installations [19]. The increasing conductor temperatures of underground cables under steady state conditions are assessed using IEC 60287 standards at 100% loading factors [20]. Ampacity is widely recognized as a vital aspect of cable design and is influenced by structural parameters, soil thermal properties, burial depth, and harmonic distortion [21, 22]. When conductor temperatures exceed permissible limits, insulation aging accelerates, significantly shortening the cable's lifespan [23]. Numerous studies in the literature investigate changes in ampacity for cables buried either directly or in thermally backfilled soil, using flat or trefoil arrangements [24]. Previous research [25-27] has examined how different parameters—such as proximity to steam pipes, alternative backfill materials, and ambient air temperature—affect cable performance. A. Cichy et al. [23, 28] optimized installation parameters for both flat and trefoil arrangements using genetic algorithms (GA). Sakis Meliopoulos and his team [29, 30] proposed mathematical models to estimate harmonic losses in cable loading. Several researchers have employed different techniques to calculate conductor resistance, cable temperature, and ampacity in the presence of harmonics [31, 32]. Judah et al. emphasized the need to account for harmonic effects when calculating ampacity for underground cables to ensure both accuracy and safety [33, 34]. High-reliability active harmonic filters that comply with IEEE 519 and EN-50160 standards represent one of several approaches to mitigate the impact of harmonics on power systems [35].

This study aims to evaluate the thermal impact of harmonics on underground power cables at the Zummar substation through a real-life case study involving five cables arranged in a configuration of three at the bottom and two at the top. It was observed that the middle bottom cable, which supplies power to an industrial zone, experiences a total harmonic distortion (THD) of 23.8%, resulting in a thermal imbalance that affects adjacent cables. This research seeks to thoroughly analyze this phenomenon using numerical thermal modeling, addressing a notable gap in the current literature concerning the localized effects of harmonics in asymmetrical cable configurations and their overall thermal performance.

2. Methodology

Three-phase Fanar-type subterranean power lines constructed at the Zummar 33/11 kV substation were the subject of an analytical investigation. As shown in Fig. 1, the system is made up of five cables, and operating at a nominal voltage of 11 kV.

A copper conductor, XLPE insulation, copper screen, PVC bedding, aluminum tape shield, and an

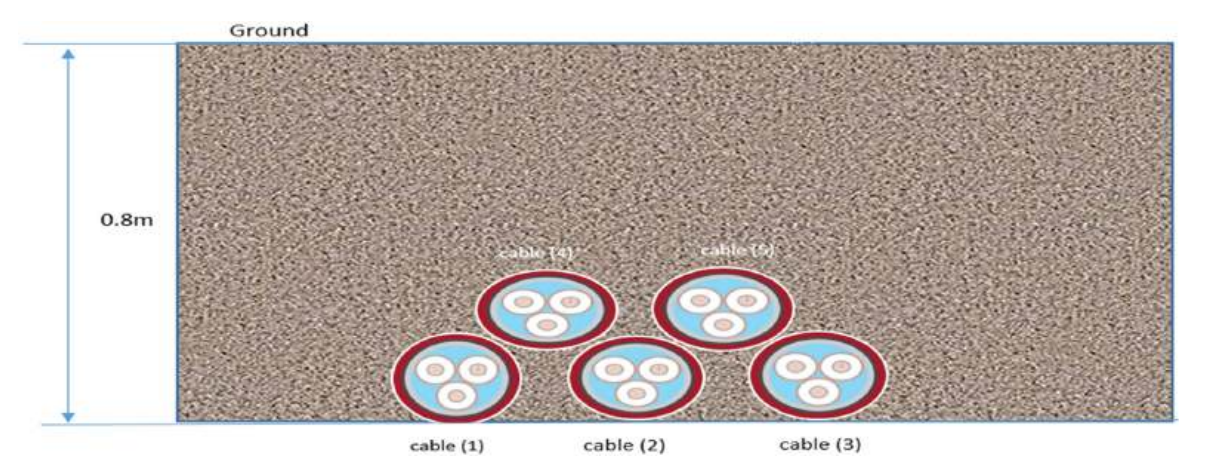


Fig. 1. Power cable in Zummar substation.

outer protective PVC sheath are among the nine main layers of the cables' multi-layered design, and they are all buried straight into the earth.

This study focuses on cables that are placed in a non-standard geometric configuration—that is, in close proximity to one another within a narrow underground trench—without adhering to globally recommended spacing guidelines. The system's thermal performance and operational safety are affected by the mutual thermal influence created by the proximity of the cables, which leads to cumulative heat buildup and elevated operating temperatures, even under rated current conditions. Additionally, one of the five cables supplies power to an industrial region with nonlinear electrical loads, including rectifiers and variable-speed drives. Field tests confirmed that this particular cable exhibits a total harmonic distortion (THD) of up to 23.3%. Due to skin and proximity effects, these harmonic currents introduce higher-frequency components that significantly increase power losses. Consequently, the temperature of the harmonic-loaded cable rises noticeably compared to the others. This scenario highlights the importance of integrating conventional thermal analysis with harmonic effect assessment when evaluating underground cable performance in real-world scenarios—particularly in complex configurations such as those found in industrial feeders and secondary substations.

To analyze heat transfer from the conductor through the cable layers and into the surrounding soil, the heat conduction equation is solved using the finite element method (FEM). The two-dimensional heat conduction model used in this study is based on the heat diffusion Eq. (1), as described in the literature [36, 37].

Where:

$$\frac{d}{d_{x}}\left(\mathbf{K}\frac{dT}{d_{x}}\right) + \frac{d}{d_{y}}\left(\mathbf{K}\frac{dT}{d_{y}}\right) + \mathbf{Q} = \rho\mathbf{c}\frac{dT}{d_{t}} \tag{1}$$

where: T is temperature in (K), x and y are spatial coordinates in (m), K is the thermal conductivity in (W/m. K), Q is the volume power of heat sources in (W/m³), ρ is the density in (kg/m³), c is the specific heat in (J/kg.K) and is the time in seconds (s).

3. Power losses in underground cables

Power losses in underground cables arise from multiple factors, primarily due to the **heat generated** within the cable structure. The main sources of these losses include:

- Conductor Losses: These occur due to the electric current flowing through the conductor, leading to Joule heating (I²R losses), which is directly proportional to the conductor resistance and current magnitude.
- Dielectric Losses: These losses result from voltage stress across the insulation, causing energy dissipation within the dielectric material. The extent of dielectric losses depends on the operating voltage and insulation properties.
- Sheath and Eddy Current Losses: These are induced by circulating currents and eddy currents in the metallic sheath and armor, which contribute to additional heat generation and affect the thermal performance of the cable system [11, 38].

Accurately evaluating these losses is essential for improving the **efficiency**, **thermal performance**, **and operational reliability** of underground power cables.

3.1. AC conductor losses

The **DC resistance** of a conductor is determined using Eq. (2)

Rdc =
$$\frac{1.02 \times 10^6 \rho_{20}}{Ac} [1 + \alpha 20) (Tc - 20)$$
 (2)

Where: ρ 20 is conductor resistivity at 20°C, α 20 is temperature coefficient at 20°C, where Ac is the conductor's cross-sectional area in millimeters and Tc is the conductor temperature in degrees Celsius.

It only gives the precise resistance value when the current is evenly dispersed across the conductor. In the case of direct current (DC), this requirement is rigorously satisfied.

However, in alternating current (AC) systems, the effective resistance of the conductor increases due to the skin effect and proximity effect. The skin effect causes the current to concentrate near the conductor's surface, reducing the effective cross-sectional area available for conduction. Additionally, the proximity effect occurs when conductors are placed close to each other, leading to uneven current distribution due to electromagnetic interactions [11, 38].

These phenomena contribute to higher resistance in AC conductors in Eq. (3), influencing power losses and the thermal performance of underground cables.

$$Rac = Rdc (1 + ys + yp)$$
 (3)

The skin effect factor ys and the proximity effect factor yp can be calculated as in [11, 38].

The volume power of heat source for each conductor (c) could be estimated as follows:

$$Qc = \frac{IB^2Rac}{Ac}, Ac = \pi r^2$$
 (4)

Where: IB is the RMS base current value (A), Ac is the cross sectional area of the conductor (m2), and Ac is the radius of the conductor (m)

3.2. Dielectric loss

The dielectric bears significant dielectric losses. Dielectric loss is influenced by voltage and becomes significant at voltage levels corresponding to the properties of the insulation material. The heat generation per unit volume within the insulation (Qd) is determined using the following Eq. (5) [39, 40].

Qd =
$$\frac{2\pi f \text{CUo}^2 \tan \delta}{\text{Ains}}$$
, Ains = $\pi r (r_{ins}^2 - \text{rc}^2)$ (5)

capacitance of the insulation (F), Uo is the phase operating voltage (V), $\tan \delta$ is the loss factor of the insulation at power frequency and operating temperature, Ains is the insulation area (m2), and rins is the outer radius of the insulation (m).

3.3. Sheath loss

Sheath loss is the result of losses in the sheath or screen brought on by the loss ratios of circulation currents (λ') and eddy currents (λ'') [39]. Shows how to calculate λ' and λ'' for sheaths that are cross-bonded or single-point bonded. The sheath's heat source's volume power (Qs) equals

$$Qs = \frac{\left(\lambda' + \lambda''\right) \times IB \ 2Rac}{Ash}, \ Ash = \pi r \left(r_{sh}^2 - r_{ins}^2\right)$$
(6)

where: Ash is the sheath area (m2), rsh is the outer radius of the sheath (m), λ' and λ'' can be calculated as in [40].

The heating of cable lines has been the subject of dozens of research papers in recent years. The thermal characteristics of analytical and numerical studies of high- and medium-voltage cables have been conducted [41, 42] and [42–44]. Power cable heat analysis has used numerical techniques like the finite element and finite difference methods.

Several studies have focused on power cables buried in the ground or installed in tunnels [45, 46]. In calculations found in the literature, power losses

generated in the cable conductor are typically determined using Joule's law for AC resistance, without considering the effect of the surrounding soil in which the cable is buried [47].

Soil properties play a crucial role in the thermal performance of underground power cables, as they influence heat dissipation resulting from the current flow in the cable. This, in turn, affects the cable's temperature and its long-term performance. Therefore, the influence of soil must be included in an accurate thermal analysis of electrical lines. Usually, these impacts are taken into account by adding particular parameters to the computational model. This approach, which is popular, is the simplest way to include the previously described impacts in thermal calculations [42–44]. The method suggested in this study, on the other hand, is predicated on the application of various forms of artificial soil (backfill materials) to examine their influence on the cable's thermal behavior.

4. Theoretical model

According to IEC60287-1-1 [10, 20], to calculate the permissible current rating, it is necessary to calculate the conditions of partial soil drying and under conditions when the lesser of the two currents measured is employed, and soil dryness does not occur. For underground cables in areas without soil drying, the allowable AC rating is provided:

$$I = \frac{\Delta\theta - \text{Wd} [0.5\text{T1} + \text{n} (\text{T2} + \text{T3} + \text{T4})]}{\text{RT1} + \text{n} (1 + \lambda 1) \text{T2} + \text{nR} (1 + \lambda 1 + \lambda 2) (\text{T3} + \text{T4})} \right]^{0.5}$$
(7)

Where R is the resistance to current per unit length of the conductor at maximum operating temperature (Ω/m) , I is the current flowing in a single conductor (A), and $\Delta\theta$ is the conductor's temperature increase above ambient temperature (K).

T1, T2, T3, and T4 are the thermal resistances per unit length between a single conductor and the jacket, the bedding between the heat shield, and Wd, which is the dielectric loss per unit length of the insulation surrounding the conductor (W/m). n is the number of load-carrying conductors in the cable (equal-sized conductors carry the same load); $\lambda 1$ is the ratio of losses in the jacket to the outer service of the cable and between the cable surface and the ambient in the center (K m/W), respectively. The number of load-carrying conductors in the cable is denoted by n, where all conductors of the same size bear the same

weight. The ratios of jacket losses to total losses in all conductors in this cable are denoted by $\lambda 1$ and $\lambda 2$, respectively.

When soil partially dries out, a buried cable's allowable AC rating is assigned a

I =

$$\left[\frac{\Delta\theta - \text{Wd}\left[0.5\text{T1} + n\left(\text{T2} + \text{T3} + \text{T4}\right) + (\nu - 1)\Delta\theta_{x}\right]}{\text{R}\left[\text{T1} + n\left(\text{1} + \lambda\text{1}\right)\text{T2} + n\text{R}\left(\text{1} + \lambda\text{1} + \lambda\text{2}\right)\left(\text{T3} + \nu\text{T4}\right)}\right]^{0.5}$$
(8)

Where v is the ratio of the thermal resistivity of the dry and moist soil zones ($v = \frac{\rho_d}{\rho_w}$) ρ_d is thermal resistivity of dry soil (K.m/W) ρ_w is rise of boundary between the try and moist zones above the ambient temperature of the soil.

The thermal resistivity of moist soil θ (K·m/w), Δ x is the temperature ($\theta_x - \theta_a$) (K) θ_x is critical temperature zones (°C), and θ_a is ambient temperature (°C).

5. Impact of harmonics on cable losses

The total conductor loss of each phase at any harmonic order can be calculated using the following equations:

$$W_c(h) = I(h)^2 * r_{a.c}(h)$$
(9)

$$W_c(h) = \alpha_i^2 I_{i, fund} 2 * r_{a.c}(h)$$

$$\tag{10}$$

Where I(h) is the cable current component that contains h th harmonic order, Ii,fund is the fundamental current of the cable in RMS, and rac(h) is the AC resistance of cable conductor at the hth harmonic in (Ω/m) . It can be obtained by Eq. (11)

$$rac(h) = rdc(1 + ys(h) + yp(h))$$
 (11)

Where rdc is the DC resistance of the cable conductor at the ambient temperature in ohms per meter, Yp(h) is the proximity effect factor, $\lambda 1(h)$ is the sheath loss factor, Ys(h) is the skin effect factor, which, in IEC60287-1-2, [18] is defined as

$$Y_s(h) = \frac{X_s^4}{192 + 0.8X^4} \tag{12}$$

$$X_s^4 = \frac{8\pi f(h) k_s 10^{-7}}{r_{dc}} \tag{13}$$

Where ks is the coefficient factor of the skin effect and f (h) is the harmonic frequency at order h.

 $Y_p(h)$ is the proximity factor which is defined by IEC60287 [10, 20]

$$Y_p(h) =$$

$$\frac{X_p^4}{192 + 0.8X_p^4} \left(\frac{d_c}{S}\right)^2 \left[0.312 \left(\frac{d_c}{S}\right)^2 + \frac{1.18}{\frac{X_p^4}{192 + 0.8X_p^4} + 0.27}\right]$$
(14)

$$X_{p}^{4}(h) = \frac{8\pi f(h) k_{p} 10^{-7}}{R_{dc}}$$
 (15)

in which S is the space in meters between cables' core axes, kp is the coefficient factor of the proximity effect, $\alpha 20$ is the coefficient of conductor temperature, and θ is the conductor temperature. The dielectric loss at each harmonic order is calculated as follows:

Qd =
$$\frac{2\pi f(h) CUo^2 \tan \delta}{Ains}$$
, Ains = $\pi r(r_{ins}^2 - rc^2)$ (16)

where f(h) means the harmonic order frequency, U0 depicts the rated voltage per phase, and C represents the electrical capacitance

6. COMSOL program

COMSOL Multiphysics 6.2 is an advanced numerical simulation software based on the Finite Element Method (FEM), widely used for multi-physics modeling in engineering applications. In electrical engineering, COMSOL enables the simulation of power cables, transformers, and electromagnetic field interactions, providing insights into their performance under various operating conditions. For the thermal analysis of power cables, the software facilitates the study of temperature distribution, heat dissipation mechanisms, and the impact of surrounding soil properties, which are critical factors in ensuring efficient cable operation. By coupling electromagnetic and thermal simulations, COMSOL allows for a comprehensive evaluation of harmonic effects, dielectric losses, and soil thermal conductivity, aiding in the optimization of underground power cable design and enhancing the reliability of electrical power transmission systems.

7. Validation

7.1. First validation

A high-voltage, three-phase, single-core, 220 kV XLPE-insulated copper cable with a rated power of

			1 0		
Formation	Soil Temp (°C)	Current (A)	Conductor Temp (°C)	This Study Conductor Temp (°C)	
Flat	25	1210	87.95	87.952	
Flat	35	1120	89.26	88.92	
Trefoil	25	1210	97.674	96.6	

Table 1. Comparison of conductor temperatures between the proposed numerical model and the reference model under the same operating conditions.

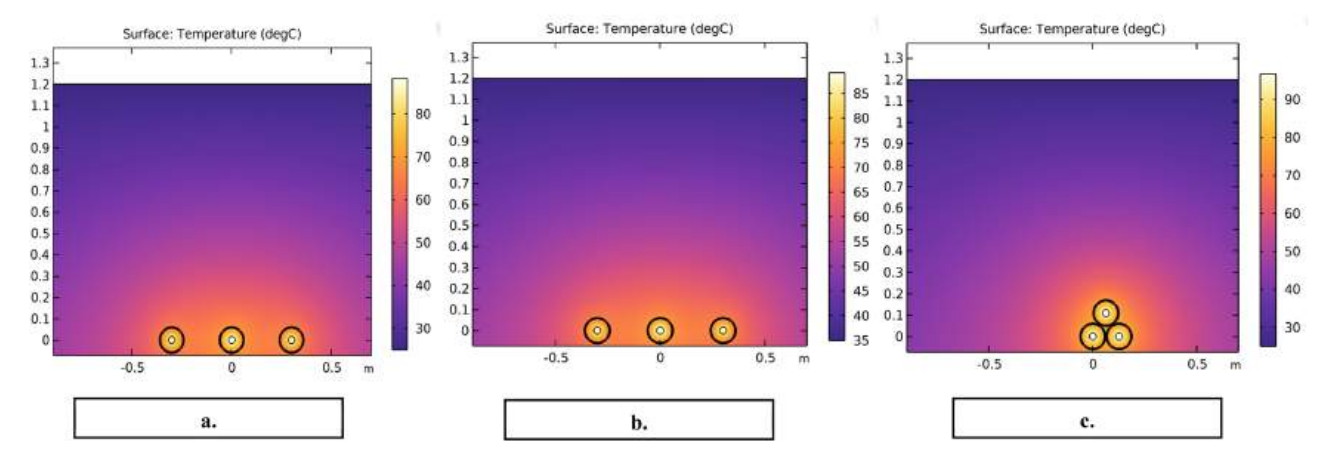


Fig. 2. This figure shows the simulated temperature distribution of the cables and soil.

- a. At load 1210A 25°C Flat Formation.
- b. At load 1120A 35°C Flat Formation.
- c. At load 1210A 25°C Tryfoil Formation.

340 MVA and a rated current of 1210 A [48] was utilized in this study to validate the model. The Egyptian-Chinese Company produced it for UHV Networks (ECC). Each cable core consists of a segmental stranded copper conductor with a nominal crosssectional area of 1200 mm². It is encased in a 4.5 mm high-density polyethylene (HDPE) outer jacket for corrosion resistance and mechanical protection, a 3 mm lead sheath, and a 25 mm thick XLPE insulation layer [48].COMSOL Multiphysics (version 6.2) was used to model the cable's thermal behavior using the heat diffusion equation and the finite element method (FEM). Automatic meshing using triangular components was applied for both flat and trefoil, configurations, and the simulation domain was set to $2.4 \text{ m} \times 2.4 \text{ m}.$

To verify the accuracy of the thermal model developed in this study, a model corresponding to the operating conditions of the reference cable mentioned above was prepared, and the obtained numerical results were compared with the published data. The results showed good agreement between the present model and the reference model, as shown in Table 1 and Fig. 2, which enhances the reliability of the adopted model in representing the thermal performance of buried power cables under various operating conditions. A comparison of conductor temperatures between the proposed numerical model and the reference model under identical conditions is provided.

7.2. Second validation

The cable data from Zummar Substation (33 kV) was obtained, along with its technical specifications from *Fanar* Cable Manufacturing Company (page 121–124) [49]. As shown in Fig. 3. The design and testing of this cable comply with the IEC 60502-2 standard, which defines the technical requirements for medium-voltage cables, including electrical, thermal, and mechanical properties, as well as material standards for insulation, shielding, and outer protection [49].

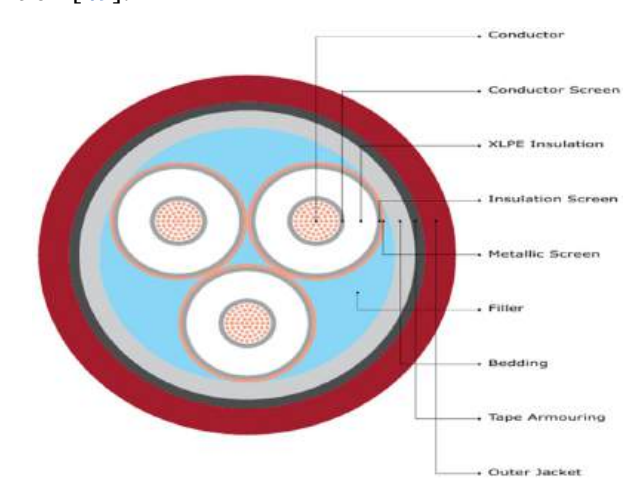


Fig. 3. The medium voltage cable cross section: 1- conductor, 2- conductor screen, 3- XLPE insulation, 4- Insulation Screen, 5- Metallic Screen, 6- Filler, 7- Bedding, 8- Tape Armouring, 9-Outer Jacket [49].

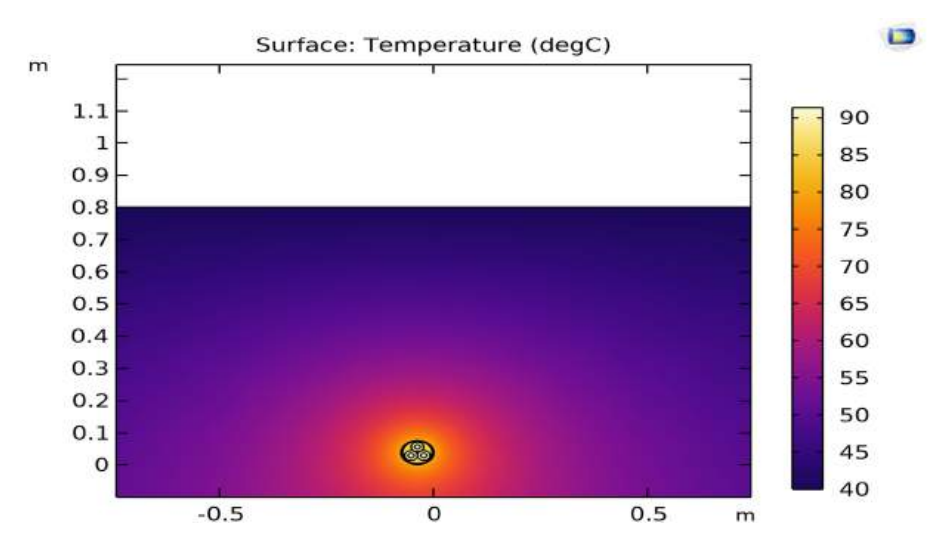


Fig. 4. Temperature distribution in different cable layers and soil at 395 A.

The manufacturer's [49] states that when the cable is buried at a depth of 0.8 meters, in soil with a thermal resistivity of 1.5 K·m/W, and under an ambient temperature of 40°C, its ampacity is 395 A. To validate this, a thermal model was developed using COMSOL Multiphasic under identical conditions. The simulation results confirmed that the allowable current closely matched the catalog value, as illustrated in Fig. 4, thereby verifying the accuracy of the thermal modeling approach.

8. Results and discussions

When underground power cables are operated, heat is generated within the electrical conductors and then transmitted through the various cable layers to the surrounding environment. Heat distribution in the soil depends on several factors:

- I. The Effect of Cable Proximity
- II. The Impact of Cable Burial Methods
- III. Thermal conductivity of backfill materials
- IV. Cable burial depth.
- V. Electrical Load.

The proximity of power cables significantly impacts their electrical performance. When multiple cables are installed closely in a flat formation, mutual heating effects occur, which reduce the current-carrying capacity (ampacity) of each cable. Previously, a single three-core cable buried at a depth of 0.8 meters in soil with a thermal resistivity of 1.5 K·m/W and under an ambient temperature of 40°C had an ampacity of 395 A. However, after adding two more cables in a flat arrangement under the same installation conditions, the ampacity of each cable decreased to 300 A due to the proximity effect. As shown in the Fig. 5.

Further assess the impact of spatial arrangement on thermal performance; a non-uniform five-cable configuration was simulated under the same loading and environmental conditions shown in Fig. 6. The cables were arranged in two vertical layers, with three cables at the bottom and two cables directly above, forming a compact cluster similar to arrangements used in field installations. The horizontal spacing between the three bottoms cables was set to 0.1 m. while the vertical distance between layers was minimized, simulating realistic installation constraints.

All cables were subjected to identical operating conditions: 0.8 meters of burial depth, a soil thermal resistivity of 1.568 K·m/W, and an ambient temperature of 32°C.

Due to the reduced spacing and lack of airflow, the simulation results indicated significant thermal interaction between the cables. The system's effective ampacity decreased markedly from its initial value to approximately 240 A per cable, as shown in the Fig. 7, because of mutual heating, which substantially raised the conductor temperatures across the group.

This finding confirms that cable layering and tight spacing drastically affect heat dissipation and thermal stability. Such configurations require careful derating and possibly enhanced thermal mitigation strategies (e.g., thermal backfill, spacing optimization) to maintain operational safety and avoid exceeding the thermal limit of the cable insulation.

8.1. Case study

The Zummar 33/11 kV substation, which had an actual operational current of 160 A per cable, provided the data in the spring. At a burial depth of 0.8 meters, with a soil thermal resistance of 1.568 kW and an ambient temperature of 32°C, the thermal

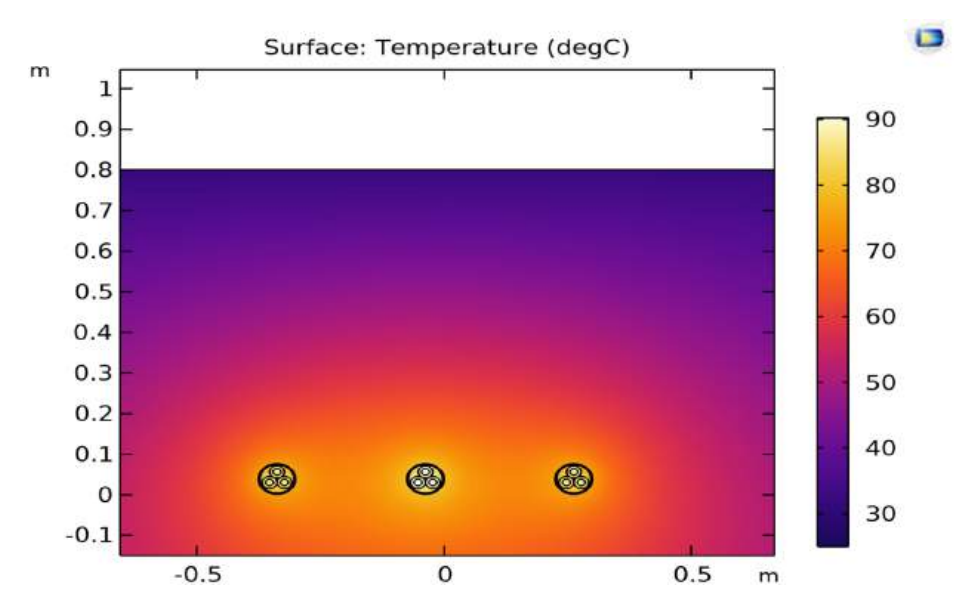


Fig. 5. Distribution Temperature for 3-cables in a flat at load 395 A.

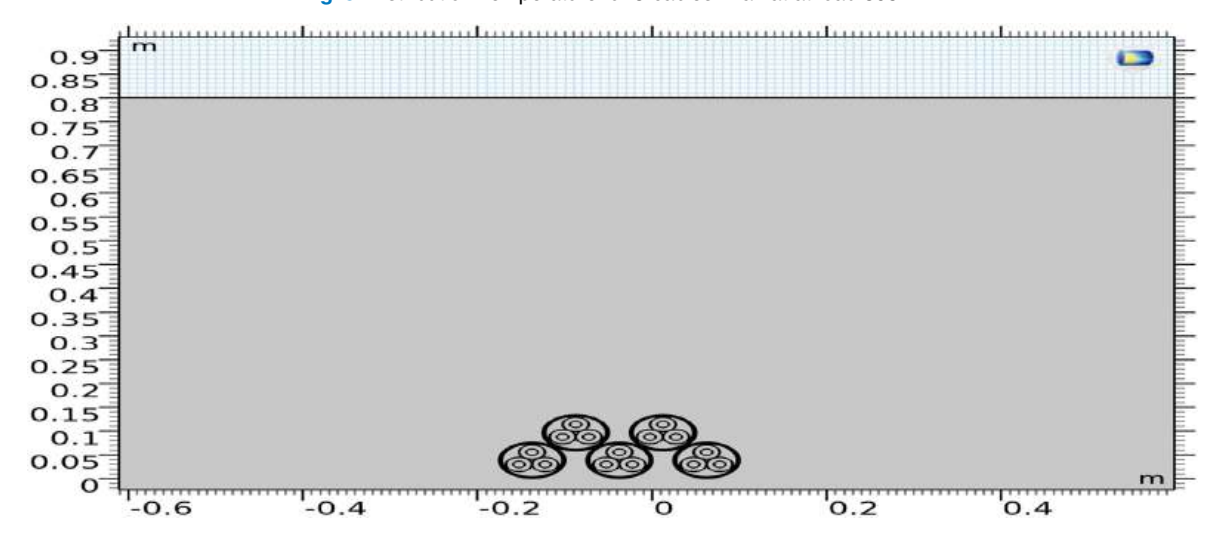


Fig. 6. Arrangement of cables 5 at depth 0.8 m.

model was recalculated using the same soil parameters and matching engineering requirements for the five-cable layout at the Zummar 33/11 kV substation. The purpose of the simulation was to confirm that the system stayed below safe temperature limits and assess the real thermal behavior under typical loading situations.

Thermal differences were observed among the five cables, mainly due to an improper geometric arrangement and mutual heating effects affecting the temperature distribution. The cable positioned at the center of the bottom layer (Cable 2) recorded the highest temperature, reaching 57.138°C, as show in Fig. 8a. This is most likely because it is improperly surrounded by other cables and soil on all sides, restricting heat dissipation and resulting in greater

thermal accumulation. As part of the field-based validation of the thermal model, operational data from Zummar 33/11kV substation revealed that Cable No. 2, located in the upper layer of the five-cable group, is currently feeding an industrial area. Measurements taken on-site confirmed that the current waveform in this cable exhibits a total harmonic distortion (THD) of 23.8%, due to the presence of nonlinear industrial loads such as inverters and frequency converters. As shown in the results in the Table 2.

Despite all five cables operating under the same fundamental load of 160A, the actual RMS current in Cable 2 was elevated to approximately 167A because of the harmonic content. This led to an increase in conductor temperature, which reached 57.8°C for cable2 as show in Fig. 8b.

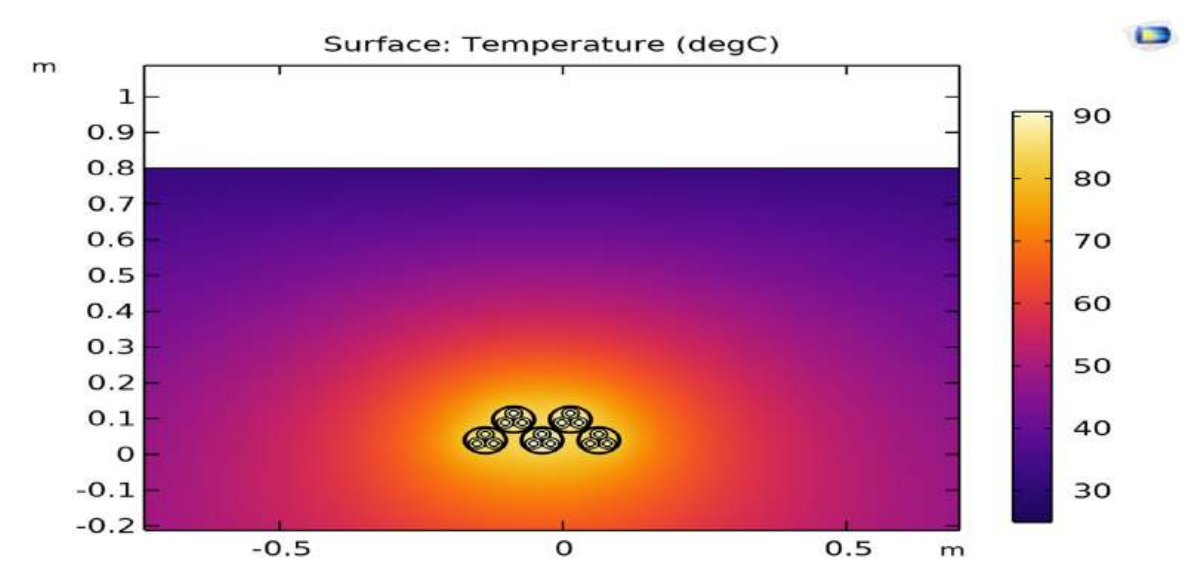


Fig. 7. Distribution temperature for 5 cables in a flat at a load of 240 A.

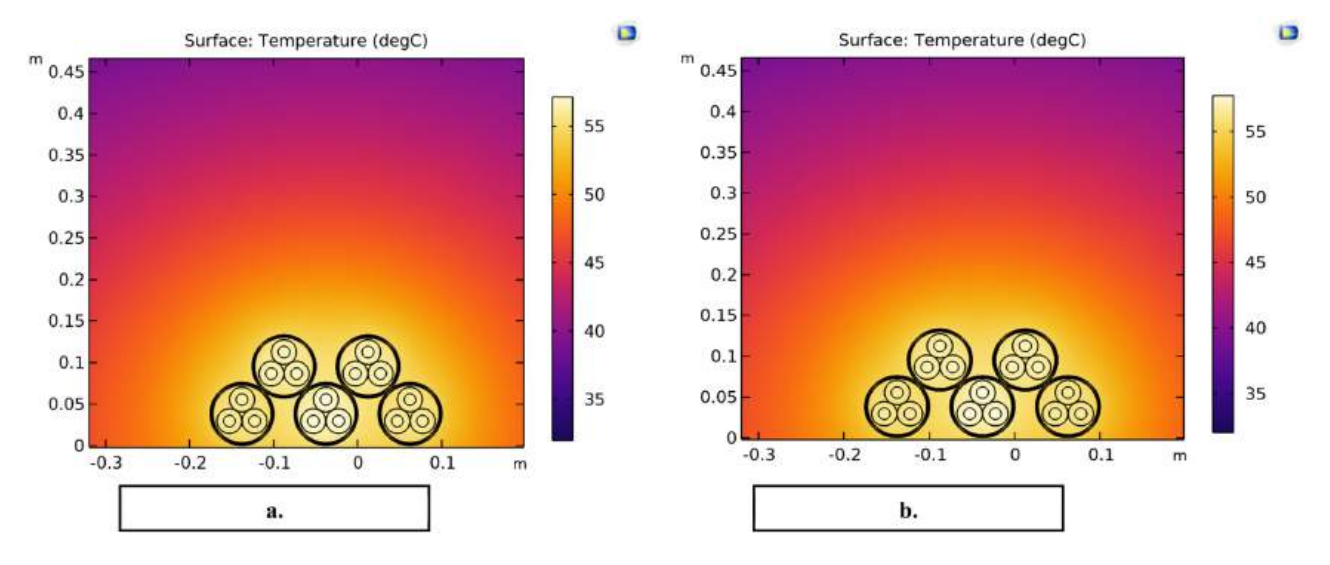


Fig. 8. Predicted temperature for 5-cables at 160 A, 32°C.a. Without harmonic.b. With harmonic.

Table 2. Cable temperature at Load 160 A wuth and without Harmonic.

Without Harmonic		With Harmonic	
Cables	Temprature (°c)	Cables	Temprature (°c)
Cable (1)	56.177	Cable (1)	56.654
Cable (2)	57.138	Cable (2)	57.8
Cable (3)	56.122	Cable (3)	56.506
Cable (4)	56.638	Cable (4)	57.047
Cable (5)	56.661	Cable (5)	57.069
	Cables Cable (1) Cable (2) Cable (3) Cable (4)		Cables Temprature (°c) Cables Cable (1) 56.177 Cable (1) Cable (2) 57.138 Cable (2) Cable (3) 56.122 Cable (3) Cable (4) 56.638 Cable (4)

8.2. Case study (2)

Due to a rise in household, industrial, cooling, and other loads, the loads on these cables went from 160 A

to around 200 A during the summer, when the outside temperature rose to about 50°C. At a burial depth of 0.8 meters, with a soil thermal resistance of 1.568 kW and an ambient temperature of 50°C, the thermal model was recalculated using the same soil parameters and matching engineering requirements for the five-cable layout at the Zummar 33/11 kV substation. The purpose of the simulation was to confirm that the system stayed below safe temperature limits and assess the real thermal behavior under typical loading situations. The cable in the center of the subgrade (Cable 2) had the greatest temperature, measuring 89.268°C. This is probably because other cables on all sides encircle it. As seen in Fig. 9a, Operational

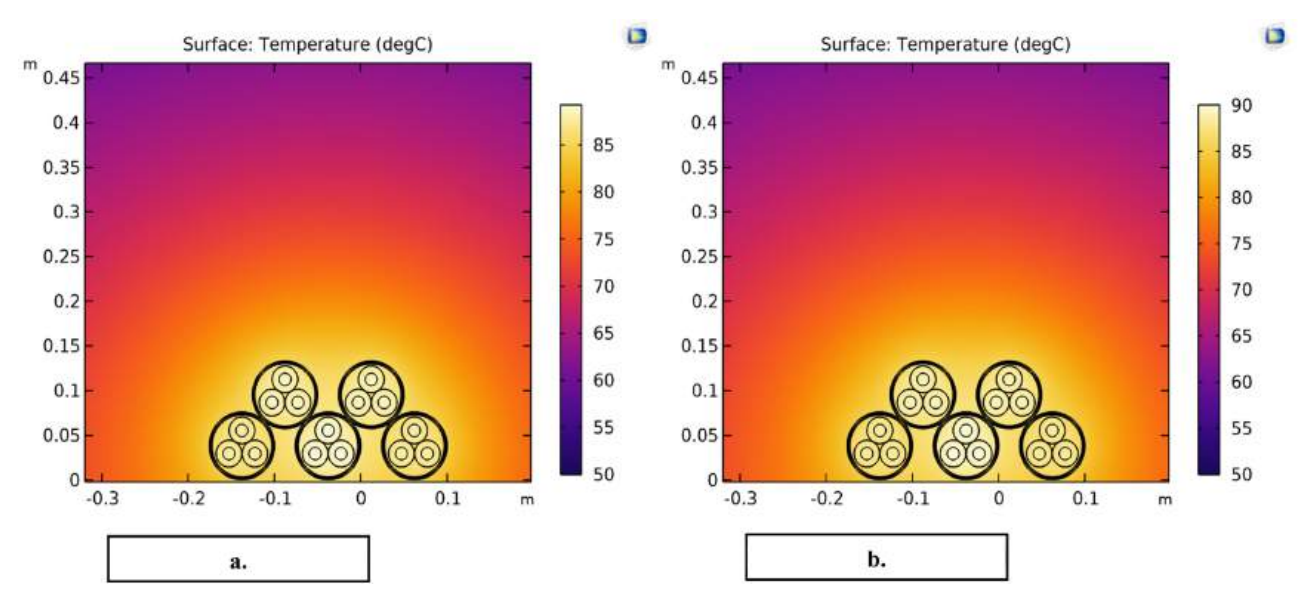


Fig. 9. Predicted temperature for 5-cables at 200 A, 50° C 44. a. without harmonic.

b. with harmonic.

Table 3. Cable temperature at Load 200 A wuth and without Harmonic.

	Without Harmonic		With Harmonic	
Load (A)	Cables	Temprature (°c)	Cables	Temprature (°c)
200 A	Cable (1)	87.77	Cable (1)	88.252
	Cable (2)	89.268	Cable (2)	90.022
	Cable (3)	87.68	Cable (3)	88.162
	Cable (4)	88.525	Cable (4)	88.988
	Cable (5)	88.548	Cable (5)	89.033

data from the Zummar 33/11 kV substation showed that Cable No. 2, which is in the upper layer of the five-cable group, is now supplying an industrial area as part of the field-based validation of the thermal model. On-site measurements verified that the presence of nonlinear industrial loads like frequency converters and inverters causes the current waveform in this cable to display a total harmonic distortion (THD) of 23.8% as shown in the results in the Table 3. Even yet; each of the five wires is subjected to the same basic 200 A load. Cables 2 has a rise in conductor temperature, reaching 90.022°C as seen in Fig. 9b.

9. Discussion

The numerical thermal modeling of the cable system at the Zummar 33/11 kV substation revealed that the non-optimal geometric arrangement of the cables—particularly their close spacing with inadequate ventilation—resulted in a significant cumulative heating effect. Due to mutual thermal interactions among cables arranged in a layered configuration (three cables in the bottom layer

and two in the top layer), the simulation indicated a considerable reduction in the effective current-carrying capacity (ampacity) from the rated design values to approximately 240 A per cable.

Both simulation and field measurements confirmed that the middle cable in the bottom layer (Cable 2) experienced the highest temperatures under all load conditions. Specifically, its temperature rose to 57.8°C during spring loading at 160 A and reached 90.02°C in summer conditions at 200 A. This elevated temperature is attributed to the cable being completely surrounded by soil and adjacent conductors, severely restricting its heat dissipation capability.

Field measurements also verified that Cable 2 supplies an industrial area with nonlinear loads, including variable-frequency drives and power converters, leading to a Total Harmonic Distortion (THD) of 23.8%. Although the fundamental current level was similar across all cables, , thereby increasing power losses and conductor temperature. Furthermore, the presence of harmonics was shown to not only impact the loaded cable but also contribute to heating of adjacent cables through thermal diffusion from the harmonically loaded conductor. This partial thermal redistribution emphasizes the importance of understanding cumulative thermal effects in densely packed underground cable installations.

10. Conclusion

The study demonstrated that the five underground cables at the Zummar substation were arranged asymmetrically in layers, and that this configuration—

combined with high harmonic distortion in one cable supplying an industrial load—resulted in significant thermal rise affecting the overall performance of the cable system. The effective current-carrying capacity was reduced, and conductor temperatures increased due to mutual thermal interactions, particularly in Cable 2 with a THD of 23.8%.

The results also revealed that harmonic effects caused partial thermal redistribution within the cable cluster, indirectly increasing the temperature of adjacent cables. This suggests that peak temperatures could be reduced by strategically shifting harmonic loads to cables experiencing lower thermal stress, such as those located in upper layers.

Additionally, the study showed that increasing the spacing between cables to 0.3 meters significantly improved thermal performance, underscoring the critical role of spatial arrangement in cable layout design.

These findings highlight the necessity of combining traditional thermal analysis with harmonic effect assessment in the design and installation of underground cable systems, especially in substations subjected to substantial nonlinear loads. Future work is recommended to include real-time temperature monitoring and transient thermal modeling to enhance long-term system reliability.

References

- H. Orton, "History of underground power cables," *Electr. Insul. Mag.*, vol. 29, pp. 52–57, 2013.
- I. Sarajcev, M. Majstrovic, and I. Medic, "Calculation of losses in electric power cables as the base for cable temperature analysis," in WIT Transactions on Engineering Sciences; WIT Press: Southampton, UK, 2020, vol. 27, pp. 529–537.
- 3. P. Ocło'n, M. Bittelli, P. Cisek, E. Kroener, M. Pilarczyk, D. Taler, R.V. Rao, and A. Vallati, "The performance analysis of a new thermal backfill material for underground power cable system," *Appl. Therm. Eng.*, vol. 108, pp. 233–250, 2016.
- 4. H. Orton, "History of underground power cables," *Electr. Insul. Mag.*, vol. 29, pp. 52–57, 2013.
- V. Goga, J. Paulech, and M. Vary, "Cooling of electrical Cu conductor with PVC insulation—analytical, numerical and fluid flow solution," *J. Electr. Eng.*, vol. 64, pp. 92–99, 2013.
- P. Hyvönen, "Prediction of insulation degradation of distribution power cables based on chemical analysis and electrical measurements," *Teknillinen korkeakoulu*, 2008.
- M. Xiao-Kai, W. Zhi-Qiang, and L. Guo-Feng, "Dynamic analysis of core temperature of low-voltage power cable based on thermal conductivity," *Can. J. Electr. Comput. Eng.*, vol. 39, pp. 59–65, 2016.
- Ł. Topolski, J. Warecki, and Z. Hanzelka, "Methods for determining power losses in cable lines with non-linear load," Przeglad Elektrotechniczny, vol. 9, pp. 85–90, 2018.
- 9. H. Kocot and P. Kubek, "The analysis of radial temperature gradient in bare stranded conductors," *Przegl ad Elektrotechniczny*, pp. 132–135, 2017.

- IEC Standard 60287-2-1: Electric Cables
 – Calculation of the Current Rating
 – Part 2: Thermal Resistance
 – Section 1: Calculation of the Thermal Resistance, 1995.
- IEEE Std 835-1994, "IEEE Standard Power Cable Ampacity Tables," IEEE Power Engineering Society, New York, NY, USA, 1994.
- I. A. Metwally, A. H. Al-Badi, and A. S. Al Farsi, "Factors influencing ampacity and temperature of underground power cables," *Electrical Engineering*, vol. 95, no. 4, pp. 383–392, 2013
- P. Ocło'n, P. Cisek, D. Taler, M. Pilarczyk, and T. Szwarc, "Optimizing of the underground power cable bedding using momentum-type particle swarm optimization method," *Energy*, vol. 92, pp. 230–239, 2015.
- P. Ocłoń, P. Cisek, M. Rerak, D. Taler, R.V. Rao, A. Vallati, and M. Pilarczyk, "Thermal performance optimization of the underground power cable system by using a modified Jaya algorithm," *International Journal of Thermal Sciences*, vol. 123, pp. 162-80, Jan 1, 2018.
- Si Fu and Y. Quan, "Numerical study of heat transfer in trefoil buried cable with fluidized thermal backfill and laying parameter optimization," *Engineering*, doi: 10.1155/2019/4741871.
- E. Kroener, A. Vallati, and M. Bittelli, "Numerical simulation of coupled heat, liquid water and water vapor in soils for heat dissipation of underground electrical power cables," *Applied Thermal Engineering*, vol. 70, no. 1, pp. 510-23, Sep 5, 2014.
- M. Altinay, "Modeling of buck type pulse width modulation (PWM) rectifier with generalized state space averaging method," Ph.D. Thesis, Kocaeli University Enstitute of Sciences, izmit, 2005.
- Currents, Power Delivery IEEE Transactions, 22 (2007), 584–594. [6], J. Desmet, et al., "Simulations of losses in LV cables due to nonlinear loads," Power Electronics Specialists Conference, PESC 2008, IEEE Conference, 2008, 785–790.
- S. M. Halpin, "Comparison of IEEE and IEC harmonic standards," in *IEEE Power Engineering Society General Meeting*, 2005, IEEE, 2005, pp. 2214–2216.
- 20. IEC Publication 60287, "Electric cables-calculation of the current rating-part 2-1,"
- M. Rerakand and P. Ocło´n, "Thermal analysis of underground power cable system," *Journal of Thermal Science*, vol. 26, no. 5, pp. 465–471, 2017.
- P. Ocło´n, P. Cisek, and M. Rerak et al., "Thermal performance optimization of the underground power cable system by using a modified Jaya algorithm," *International Journal of Thermal Sciences*, vol. 123, pp. 162–180, 2018.
- A. Cichy, B. Sakowicz, and M. Kaminski, "Economic opti mization of an underground power cable installation," *IEEE Transactions on Power Delivery*, vol. 33, no. 4, pp. 1124–1133, 2018.
- S. Czapp and F. Ratkowski, "Optimization of Thermal backfill configurations for desired high-voltage power cables ampacity," *Energies*, vol. 14, p. 1452, 2021.
- D. Enescu, P. Colella, and A. Russo, "Thermal assessment of power cables and impacts on cable current rating: An overview," *Energies*, vol. 13, p. 5319, 2020.
- R. Masnicki, J. Mindykowski, and B. Palczynska, "Experiment-based study of heat dissipation from the power cable in a casing pipe," *Energies*, vol. 15, p. 4518, 2022.
- 27. H. Brakelmann, G. J. Anders, and P. Zajac, "Fundamentals of the thermal analysis of complex arrangements of underground heat sources," *Energies*, vol. 14, p. 6813, 2021.
- A. Cichy, B. Sakowicz, and M. Kaminski, "Detailed model for calculation of life-cycle cost of cable ownership and comparison with the IEC formula," *Electric Power Systems Research*, vol. 154, pp. 463–473, 2018.

- A. P. Sakis Meliopoulos and M. A. Martin Jr., "Calculation of secondary cable losses and ampacity in the presence of harmonics," *IEEE Trans Power Del*, vol. 7, no. 2, pp. 451–457, 1992.
- J. H. Neher and M. H. McGrath, "The calculation of the temperature rise and load capability of cable systems," *AIEE Trans.*, vol. 76, pp. 752–772, 1957.
- 31. J. Nahman and M. Tanaskovic, "Determination of the current carrying capacity of cables using the finite element method," *Electr Power Syst Res.*, vol. 61, pp. 109–117, 2002.
- B. Park, J. Lee, H. Yoo, and G. Jang, "Harmonic mitigation using passive harmonic filters: Case study in a steel mill power system," *Energies*, vol. 14, p. 2278, 2021.
- D. Lumbreras, E. Gálvez, A. Collado, and J. Zaragoza, "Trends in power quality, harmonic mitigation and standards for light and heavy industries: A review," *Energies*, vol. 13, p. 5792, 2020.
- 34. K. B. Nazirov, Z. S. Ganiev, S. D. Dzhuraev, S. T. Ismoilov, and R. A. Rahimov, "Elaboration of the method for providing the level of power quality in the nodes of the energy system while power quality monitoring," in *Proceedings of the 2020 IEEE* Conference of Russian Young esearchers in Electrical and Electronic Engineering, EIConRus, 2020, St. Petersburg and Moscow, Russia, January 27–30, 2020, IEEE, pp. 1282–1286, 2020.
- O. E. Gouda, "Thermal analysis of the influence of harmonics on the current capacity of medium-voltage underground power cables," *Energy Sci Eng.*, vol. 11, pp. 3471–3485, 2023.
- P. Klimenta, J. Klimenta, and K. Milovanović, "Modelling the thermal effect of solar radiation on the ampacity of a low voltage underground cable," *International Journal of Thermal Sciences*, vol. 134, pp. 507–516, 2018, doi: 10.1016/j. ijthermalsci.2018.08.012.
- Magdy B. Eteiba, Mohamed Mamdouh Abdel Aziz, and Jehan Hassan Shazly, "Heat Conduction Problems in SF₆ Gas Cooled-Insulated Power Transformers Solved by the Finite-Element Method," *IEEE Transactions on Power Delivery*, vol. 23, no. 3: pp. 1457–1463, 2008.
- J. O. Williams, "Narrow-band analyzer," Ph.D. dissertation. Department of Electronic Engineering, Harvard University, Cambridge, Massachusetts, USA, 1993.

- J. C. Whitaker, "AC Power Systems Handbook-Second edition," Boca Raton: CRCPres LLC, 1999.
- J. Blackledge, E. Coyle, and K. O'Connell, "Proximity heating effects in power cables," *IAENG Letters*, forthcoming, vol. 2013, 2013, doi:10.21427/D7HP61.
- B. Rozegnał, P. Albrechtowicz, D. Mamcarz, M. Rerak, and M. Skaza, "The power losses in cable lines supplying nonlinear loads," *Energies*, vol. 14, p. 1374, 2021.
- P. Ocło'n, M. Bittelli, P. Cisek, E. Kroener, M. Pilarczyk, D. Taler, R. V. Rao, and A. Vallati, "The performance analysis of a new thermal backfill material for underground power cable system," *Appl. Therm. Eng.*, vol. 108, pp. 233–250, 2016
- P. Ocło´n, D. Taler, and Cisek, "Fem-based thermal analysis of underground power cables located in backfills made of different materials," *Strength Mater*, vol. 47, pp. 770–780, 2015.
- Z. WenWei, Z. YiFeng, H. ZhuoZhan, W. XiangBing, W. Yan-Feng, L. Gang, X. Yue, and Z. NingXi, "Thermal effect of different laying modes on cross-linked polyethylene (XLPE) insulation and a new estimation on cable Ampacity," *Energies*, vol. 12, p. 2994, 2019.
- M. Xiao-Kai, W. Zhi-Qiang, and L. Guo-Feng, "Dynamic analysis of core temperature of low-voltage power cable based on thermal conductivity," *Can. J. Electr. Comput. Eng.*, vol. 39, pp. 59–65, 2016.
- I. Metwally; A. Al-Badi; A. Al Farsi, "Factors influencing ampacity and temperature of underground power cables," *Electr. Eng.*, vol. 95, pp. 383–392, 2013.
- Y. Wang, R. Chen, J. Li, S. Grzybowski, and T. Jiang, "Analysis of influential factors on the underground cable ampacity," in *Proceedings of the IEEE Conference on Electrical Insulation Conference, Annapolis, MD, USA*, 5–8 June 2011, pp. 430–433.
- 48. J. H. Shazly et al., "Thermal analysis of high-voltage cables with several types of insulation for different configurations in the presence of harmonics," *IET Generation, Transmission & Distribution*, vol. 11, no. 14, pp. 3439–3448, 2017.
- Alfanar, Medium Voltage Power and Special Application Cables. Alfanar Technical Catalog.